Distributed Model Predictive Control of A Wind Farm for Optimal Active Power Control

Part I: Clustering based Wind Turbine Model Linearization

Zhao, Haoran; Wu, Qiuwei; Guo, Qinglai ; Sun, Hongbin; Xue, Yusheng

Published in:
IEEE Transactions on Sustainable Energy

Link to article, DOI:
10.1109/TSTE.2015.2418282

Publication date:
2015

Document Version
Peer reviewed version

Distributed Model Predictive Control of A Wind Farm for Optimal Active Power Control Part I: Clustering based Wind Turbine Model Linearization

Haoran Zhao, *student member, IEEE,* Qiuwei Wu, *member, IEEE*, Qinglai Guo, *senior member, IEEE*, Hongbin Sun, *senior member, IEEE* and Yusheng Xue, *senior member, IEEE*

***Abstract*-This paper presents a dynamic discrete-time Piece-Wise Affine (PWA) model of a wind turbine for the optimal active power control of a wind farm. The control objectives include both the power reference tracking from the system operator and the wind turbine mechanical load minimization. Instead of partial linearization of the wind turbine model at selected operating points, the nonlinearities of the wind turbine model are represented by a piece-wise static function based on the wind turbine system inputs and state variables. The nonlinearity identification is based on the clustering-based algorithm, which combines the clustering, linear identification and pattern recognition techniques. The developed model, consisting of 47 affine dynamics, is verified by the comparison with a widely-used nonlinear wind turbine model. It can be used as a predictive model for the Model Predictive Control (MPC) or other advanced optimal control applications of a wind farm.**

***Index Terms*-Clustering based identification, model predictive control (MPC), piece wise affine (PWA) model, wind turbine.**

I. Introduction

WIND energy has developed rapidly in the past 20 years and has a leading role among renewable energies. By the end of 2013, there was 117.3 GW of installed wind energy capacity in Europe: 110.7 GW onshore and 6.6 GW offshore. The electricity produced by the wind energy is enough to cover around 8% of the EU's total electricity consumption [1].

With the increasing wind power penetration level, the wind farm is required to be more controllable to meet the more stringent technical requirements specified by system operators, including active power control [2]. At the wind farm level, the requirements specify different types of active power control: absolute power limitation, delta limitation, balance control, etc. [3]. The power references are assigned to each turbine according to the distribution algorithm of the wind farm control system. At the wind turbine level, a pitch angle reference and a generator torque reference are computed based on the power reference and given to the actuating subsystems. With the development of power electronics, the dynamic response and controllability of modern Variable Speed Wind Turbines (VSWTs) have been largely improved [4], [5].

For the active power set-points to individual wind turbines, instead of simple proportional distribution, multi-objective distribution algorithms have been developed, which are to dynamically distribute active power set-points in order to minimize the mechanical loads experienced by the turbines while maintaining the desired power production at all times [6]- [8]. The role of individual wind turbines is an actuator which operates at the derated condition and aims to generate power according to the reference value derived from the wind farm control. The wind turbine control is considered as fixed and known. The power controlled wind turbine model, proposed in [9], is adopted in this paper and shown in Fig. 1. The power reference $P_{\mathrm{ref}}^{\mathrm{WT}}$ and wind speed v_{w} are the inputs. For the output signals, besides the output power (P_{g}), shaft torque (T_{s}) and thrust force (F_{t}) are included to evaluate wind turbine mechanical load. F_{t} and T_{s} affect the wind turbine tower structure and gearbox, respectively. The oscillatory transient of F_{t} leads to undesired nodding of the tower and causes fatigue of the wind turbine. The torsional torque T_{s} is transferred through gearbox, which is the vulnerable part of the wind turbine. The oscillatory transient of T_{s} creates micro cracks in the material which can further lead to the component failure.

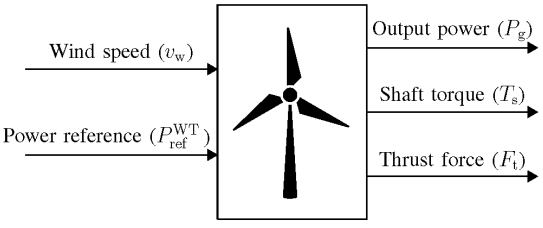

Fig. 1 Power controlled wind turbine [9]

The work was supported by the Sino-Danish Centre for Education and Research (SDC) through the PhD project of "Coordinated Control of Wind Power Plants and Energy Storage Systems" and National Key Basic Research Program of China (973 Program)(2013CB228201).

H. Zhao is with Center for Electric Power and Energy, Department of Electrical Engineering, Technical University of Denmark, Kgs. Lyngby, 2800, Denmark, and Sino-Danish Center for Education and Research, Aarhus, 8000 Denmark (email: hzhao@elektro.dtu.dk).

Q. Wu is with Center for Electric Power and Energy, Department of Electrical Engineering, Technical University of Denmark, Kgs. Lyngby, 2800, Denmark, and Sino-Danish Center for Education and Research, Aarhus, 8000 Denmark, and State Key Lab. of Power System, Dept. of Electrical Engineering, Tsinghua University, Beijing 100084, China (email: qw@elektro.dtu.dk).

Q. Guo and H. Sun are with Department of Electrical Engineering, Tsinghua University, Beijing 100084, China (email: guoqinglai@tsinghua.edu.cn, shb@mail.tsinghua.edu.cn).

Y. Xue is with State Grid Electric Power Research Institute, Nanjing, 210003, China (e-mail: xueyusheng@sgepri.sgcc.com.cn).

The aforementioned power controlled wind turbine model is a strong coupling, high-order nonlinear model. The operating point shifts from time to time according to the power reference and wind speed. Therefore, the controller designed for a specific operating point cannot guarantee the control performances within the whole operating range. For applying advanced control strategies, such as Model Predictive Control (MPC) and Linear Quadratic Regulator (LQR), the model should be a discrete-time piecewise affine (PWA) model which covers the entire operating regime.

Due to the multiple state and input variables of the wind turbine system, the operating points are multidimensional. In most references, the nonlinearities are approximated using the first-order Taylor series approximation at various operating points [9]-[11]. However, the whole operating regime is partitioned only based on the wind speed, and the impacts of other state and input variables are not taken into account. The main challenge of the identification of PWA models involves the estimation of both the parameters of the affine sub-models, and the coefficients of the polytopes defining the partition of the regressor (state+input) set [12].

Identification methods for PWA systems have been proposed in many publications [13]-[17]. A gridding procedure of the regressor set was proposed in [13], where the domain of the nonlinearity was uniformly divided into a number of simplices. Similar approach was also reported in [14]. This approach simplifies the region estimation. However, the number of small regions grows exponentially with the system dimension and it is impractical to use it for high-dimensional systems. In [15], [16], the identification of PWA models was formulated as a Mixed Integer Quadratic Program (MIQP). The global optimum could be obtained. The drawback of this approach is that the computation complexity grows polynomially with the number of data. To cope with the problem, a novel algorithm combining clustering, pattern recognition and linear identification techniques was developed in [17] whose advantage is the procedure that transforms the problem of classifying the data to an optimal clustering problem. It is adopted to identify the PWA wind turbine model in this paper.

To the knowledge of the authors, only a few studies have been conducted on the identification of a PWA wind turbine model. In [18], this clustering based method was used for identifying the wind turbine model for local wind turbine control. The inputs are generator torque $T_{\mathrm{g}}^{\mathrm{ref}}$ and pitch angle reference θ_{ref} . Identification was performed around the optimal static characteristic of wind turbine.

Unlike [18], this paper focuses on the identification of a PWA wind turbine model for the wind farm control application. The developed wind turbine model has power reference $P_{\mathrm{ref}}^{\mathrm{WT}}$ and wind speed v_{w} as inputs, and output power, shaft torque and thrust force as outputs which well fits the wind farm control architecture. The nonlinear control loops including the generator torque control and the pitch angle control are embedded in the model and are identified. Identification was performed in the whole derated operation regime of the wind turbine.

The paper is organized as follows: Section II describes the operation areas of the power controlled wind turbine. The clustering-based method for system identification is discussed in Section III. The nonlinear wind turbine model is presented in Section IV, which is identified and transformed into a discrete PWA model in Section V. Case studies for verifying the developed PWA wind turbine model are presented and discussed in Section VI. The conclusion is drawn in the end.

II. Operation Areas of a Power Controlled Wind Turbine in A Wind Farm

The wind turbine model developed by National Renewable Energy Laboratory (NREL) [19] is widely used to represent a variable speed pitch-controlled wind turbine, which is adopted in this paper. It consists of several subsystems, including aerodynamics, drive train, tower, generator, pitch actuator and the wind turbine controller, as shown in Fig. 2. According to the control strategy described in [20], based on the power reference $P_{\mathrm{ref}}^{\mathrm{WT}}$ generated from the wind farm controller, a pitch angle reference θ_{ref} and a generator torque reference $T_{\mathrm{g}}^{\mathrm{ref}}$ are computed and sent to the pitch controller and the generator torque controller, respectively.

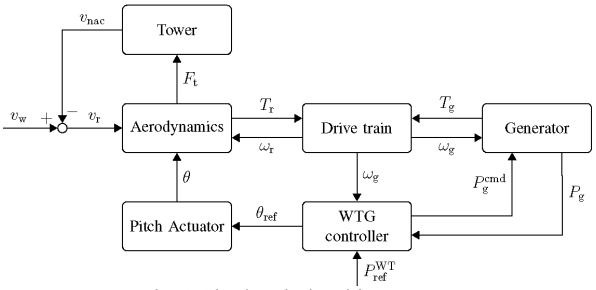

Fig. 2 Single wind turbine system

The wind turbine control objectives vary according to different wind conditions [21]. When the wind speed v_{w} is larger than the nominal value, the wind turbine controller aims to limit the captured wind power to the rated power ($P_{\mathrm{ref}}^{\mathrm{WT}} = P_{\mathrm{rated}}$) by regulating the pitch angle to prevent the generator speed ω_{g} from over-speeding. When v_{w} is less than the nominal speed, the controller will extract maximum available wind power ($P_{\mathrm{ref}}^{\mathrm{WT}} = P_{\mathrm{avi}} \le P_{\mathrm{rated}}$) by fixing the pitch angle ($\theta = 0$) and adjust the generator torque to track the optimal rotor speed. The optimal regimes characteristic (ORC) is plotted in the $\omega_{\mathrm{r}} - \theta - v_{\mathrm{w}}$ space, as shown in Fig. 3. The polytope marked in the figure is the area where the power coefficient $C_{\mathrm{p}} > 0$.

When the wind turbine operates in the derated mode, i.e. wind turbine produces less power than the available power ($P_{\mathrm{ref}}^{\mathrm{WT}} \le P_{\mathrm{avi}} \le P_{\mathrm{rated}}$), the operation areas under steady state shall be below the ORC and can be divided into two parts according to the pitch angle (shown in Fig. 3). When the pitch angle control is activated ($\theta > 0$), the corresponding area is defined as “Area I”. In this area, the captured power is reduced by regulating the pitch angle in order to prevent the generator speed from over-speeding. Therefore, ω_{g} is always limited at its maximum value. When the pitch angle is deactivated (

$\theta = 0$), the corresponding region is defined as "Area II". In this area, the generator speed is regulated to reduce the captured power.

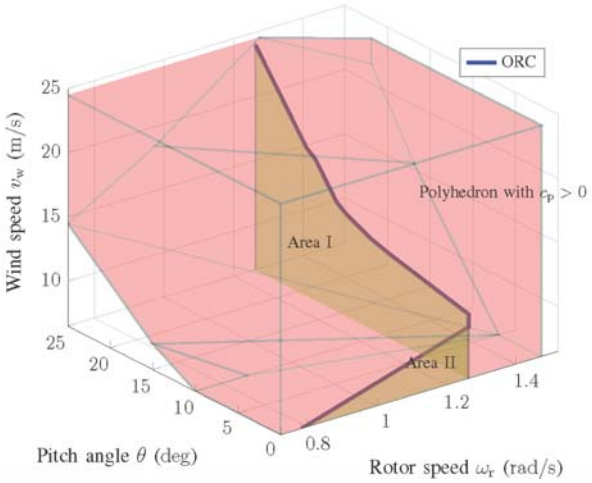

Fig. 3 Operation areas in $\omega_r - \theta - v_w$ space

In the aforementioned derated control strategy, the power reduction is realized via generator speed regulation if the pitch control is deactivated. Another widely applied derated control strategy is by regulating the pitch angle while ω_g remains below its maximum value. Various methods have been proposed for this practice [22], [23]. In this case, for any given wind speed v_w, ω_r is desired to maintain its optimal speed according to ORC. Therefore, the operation areas of this practice are different from these shown in Fig. 3.

Wind turbine with both of the derated control strategies can be identified based on the clustering based approach. As the controller equation is integrated in the wind turbine model, different derated control strategies result in different dynamic models whose nonlinearities are also different. This paper focuses on the wind turbine model with the derated control via generator speed regulation.

III. THE CLUSTERING BASED IDENTIFICATION METHOD

This section describes the procedure of the clustering based identification method. A nonlinear static function $f(x)$ can be approximated with a PWA map,

$$f(x) = \begin{cases} [x,1]\alpha^1, \text{ if } x \in \chi^1 \\ [x,1]\alpha^2, \text{ if } x \in \chi^2 \\ \vdots \\ [x,1]\alpha^s, \text{ if } x \in \chi^s \end{cases} \quad (1)$$

where x is the static function input; $f(x)$ is the output; χ represents a bounded polyhedron which is the regressor set and is partitioned into s regions; α^i denotes the affine function Parameter Vectors (PVs). The task of the identification is to reconstruct the map f based on the dataset $(f(x_k), x_k)_{k=1}^n$. The clustering-based identification method mainly consists of the following steps.

A. Building local dataset

A Local Dataset (LD) C_k collects a point $(f(x_k), x_k)$ and its nearest $c-1$ points. The distance is measured in the Euclidean metric [18]. A pure C_k refers to a LD whose outputs are generated by only one model. Otherwise, the LD is a mixed one. The cardinality c is a tuning parameter. In order to achieve good approximation results, the ratio between pure and mixed LD should be high. A small c leads to a small number of mixed points. However, to deal with the effect of noises on the accuracy of the local model, a bigger c is required. Therefore, c should be properly tuned to get the trade-off.

Accordingly, the local parameter vector α^{LS_k} is computed for each C_k through least squares. Parameter values α^{LS_k} and the mean value of the inputs m_k form the feature vector $\xi_k = [(\alpha^{LS_k})', m_{k'}]'$. ξ_k holds both information of localization of C_k and its corresponding affine model parameters. Furthermore, the variance R_k of the feature vectors is computed as a diagonal block matrix consisting of the covariance V_k of α^{LS_k} and the scatter matrix Q_k of m_k. The variance R_k is used to compute confidence measure of ξ_k.

B. Clustering algorithm

The clustering algorithm is to partition the feature vectors into s clusters $\{F_i\}_{i=1}^s$. The partition can be performed either using a supervised clustering method (K-means) or unsupervised clustering method (single-linkage). To reduce the complexity of the problem, the K-means method is adopted where s is pre-fixed. It exploits pre-computed confidence measures on feature vectors, which is used to reduce negative effects of LDs which are supposed to be mixed.

C. Submodel parameters estimation

As the local models with similar features are collected to each cluster, the data points are classified into one of the data subsets D_i using the mapping,

$$(f(u_k), u_k) \in D_i, \text{if } \xi_k \in F_i. \quad (2)$$

The submodel parameter vector α^i is estimated using weighted least squares over the data subset D_i.

D. Region estimation

In this step, the complete polyhedral partitions of the regressor set are found. Polytopes χ^i with $(i = 1,...,s)$ are decided by solving the multi-category classification problem. Different classification methods, such as Multi-category Robust Linear Programming (MRLP), Support Vector Classification (SVC) and Proximal SVC (PSVC), are introduced and compared in [24]. In this study, the optimization based MRLP is used due to its high accuracy.

IV. NONLINEAR WIND TURBINE MODEL

Due to the large sampling time t_s of the wind farm controller (normally in seconds, e.g. $t_s = 1\text{s}$ in [8]), the fast dynamics related to the electrical system is excluded in the wind turbine model. Besides, the oscillations in the shaft torsion and tower nodding are also ignored to reduce the complexity [9]. A simplified nonlinear model of the NREL wind turbine with the inputs and outputs shown in Fig. 1 is described in this section.

A. Aerodynamics

As the main source of nonlinearities, the aerodynamic torque T_a and thrust force F_t can be expressed by (3) and (4), respectively,

$$T_a = \frac{0.5\pi\rho R^2 v_r^3 C_p(v_r, \omega_r, \theta)}{\omega_r} \tag{3}$$

$$F_t = 0.5\rho R^2 v_r^2 C_t(v_r, \omega_r, \theta) \tag{4}$$

where ρ is the air density, R is the blade length, v_r is the effective wind speed on the rotor, C_p and C_t represent the power coefficient and thrust coefficient, respectively.

B. Drive train

The drive train is considered to be rigidly coupled. The rotor inertia J_r and generator inertia J_g are lumped into one equivalent mass J_t. The single-mass model represented by the low-speed shaft motion equation is used [25],

$$J_t = J_r + N_g^2 J_g \tag{5}$$

$$\dot{\omega}_r = \frac{1}{J_t}(T_a - N_g T_g) \tag{6}$$

$$\omega_g = N_g \omega_r \tag{7}$$

where N_g is the gear box ratio, ω_r and ω_g are the speed of the rotor and generator, J_r and J_g are the inertias of the rotor and generator, respectively. The shaft torque T_s twisting the low-speed shaft is computed by,

$$T_s = \frac{N_g^2 J_g}{J_t} T_r + \frac{N_g J_r}{J_t} T_g \tag{8}$$

C. Generator

To follow the power reference command P_g^{cmd} (see Fig. 2), the electrical torque T_g is regulated to follow the torque reference T_g^{ref}, obtained by the following equation,

$$T_g^{\text{ref}} = \frac{P_g^{\text{cmd}}}{\omega_g}. \tag{9}$$

The vector control is applied in the local torque control loop, which ensures a fast and accurate response. The time window of the dynamic is normally in milliseconds and therefore can be disregarded,

$$T_g \approx T_g^{\text{ref}} \tag{10}$$

The output power P_g can be derived by,

$$P_g = \mu T_g \omega_g \tag{11}$$

where μ denotes the generator efficiency. It is assumed that μ is well compensated by setting $P_g^{\text{cmd}} = \frac{P_{\text{ref}}^{WT}}{\mu}$. Accordingly,

$$P_g = P_{\text{ref}}^{\text{WT}}. \tag{12}$$

D. Tower

The swaying movement of the nacelle changes the relative wind speed on the rotor. When the tower deflection is denoted as x_t, and the effective wind speed on the rotor is computed by $v_r = v_w - \dot{x}_t$. Since the dynamics are disregarded,

$$v_r \approx v_w. \tag{13}$$

E. Pitch actuator

As proposed in [9], the dynamics and the nonlinearities of the pitch actuator are disregarded. The inertia of the pitch system is considered in the wind turbine controller design. The pitch angle θ is regulated by the gain-scheduled PI controller based on the deviation of the filtered generator speed ω_f from the rated speed ω_{rated},

$$\dot{\theta} = -\frac{K_p}{K_c}\dot{\omega}_f - \frac{K_i}{K_c}(\omega_f - \omega_{\text{rated}}) \tag{14}$$

$$-\Delta\theta_{\max} \le \dot{\theta} \le \Delta\theta_{\max} \tag{15}$$

$$\dot{\omega}_f = \frac{1}{\tau_g}\cdot\omega_g - \frac{1}{\tau_g}\cdot\omega_f \tag{16}$$

$$K_c = f_{\text{corr}}(P_{\text{ref}}^{\text{WT}}(k-1), \theta(k-1)) \tag{17}$$

where K_p and K_i represent proportional and integral gain of the PI controller, K_c indicates the correction factor which is a time-variant function of $P_{\text{ref}}^{\text{WT}}$ and θ of the previous time step ($P_{\text{ref}}^{\text{WT}}(k-1)$, $\theta(k-1)$), $\Delta\theta_{\max}$ indicates the maximum rate of change of the pitch angle, τ_g denotes the time constant of the measurement filter for the generator speed ω_g.

With (3)-(17), the nonlinear dynamics of the wind turbine model can be transformed into the following form,

$$\begin{aligned} \dot{x} &= Ax + Bg \\ y &= Cx + Dg \end{aligned} \tag{18}$$

with

$$x = \begin{bmatrix} \omega_r \\ \omega_f \\ \theta \end{bmatrix}, g = \begin{bmatrix} T_a \\ T_g \\ F_t \\ \omega_{\text{rated}} \end{bmatrix}, y = \begin{bmatrix} T_s \\ F_t \end{bmatrix},$$

$$A = \begin{bmatrix} 0 & 0 & 0 \\ \frac{N_g}{\tau_g} & -\frac{1}{\tau_g} & 0 \\ -\frac{K_p N_g}{K_c \tau_g} & \frac{K_p - K_i \tau_g}{K_c \tau_g} & 0 \end{bmatrix}$$

$$B=\begin{bmatrix} \frac{1}{J_t} & -\frac{N_g}{J_t} & 0 & 0 \\ 0 & 0 & 0 & 0 \\ 0 & 0 & 0 & \frac{K_i}{K_c} \end{bmatrix},$$

$$C=\begin{bmatrix} 0 & 0 & 0 \\ 0 & 0 & 0 \end{bmatrix}, D=\begin{bmatrix} \frac{N_g^2 J_g}{J_t} & \frac{N_g J_r}{J_t} & 0 & 0 \\ 0 & 0 & 1 & 0 \end{bmatrix},$$

where ω_{rated} is considered as fixed. The corresponding discrete-time form of the system (18) with sampling time t_s can be obtained [26],

$$\begin{aligned} x(k+1) &= A_d' x(k) + B_d' g(k) \\ y(k) &= C_d' x(k) + D_d' g(k) \end{aligned} \tag{19}$$

where A_d', B_d', C_d', D_d' are the discrete form of A, B, C, D in (18), respectively. The nonlinear parts, including T_a, F_t and T_g are identified in Section V.

It should be noticed that the relevant elements of matrix A_d' and B_d' are not fixed due to the constraint of $\dot{\theta}$ in (15) and time variant K_c. Therefore, A_d' and B_d' should be identified and updated according to the partitioned regions. They are also explained in Section V.

V. Discrete-time PWA Modeling of a Wind Turbine

Following the procedure of the clustering-based identification method, the discrete-time PWA model of a wind turbine is developed in this section.

A. Identification of aerodynamic torque T_a

Since T_a is derived by a static nonlinear function of ω_r, v_w, θ, the regressors should be located close to the operation areas (Area I and Area II in Fig. 3 in the three-dimensional space $[\omega_r, v_w, \theta]'$, limited by the constraints of ω_r, v_w, θ). Besides, sufficient regressors should be generated to have a good approximation of the nonlinear function.

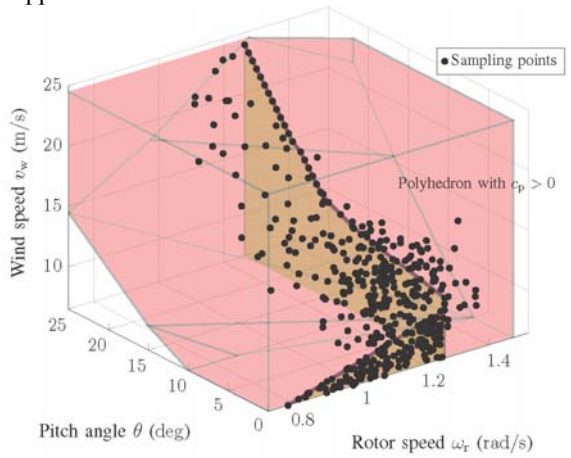

Fig. 4 Regressors for identification of T_a

Here, 1000 regressors are randomly generated with Gaussian distribution characterized with the mean value on the both operation areas and dispersion σ^2 around them, as illustrated in Fig. 4.

Accordingly, the aerodynamic torque T_a to each regressor is computed by (3) where C_p is obtained by interpolation of the look-up table in [19]. As described in Section III A and B, the region number s and the number of the points in LD c shall be pre-defined. Obviously, a larger s can have better approximation. However, it leads to the increase of computation complexity for searching and more spaces requirements for storage. In this study, $s=5$ and $c=20$ show a good approximation. The clustering-based identification is performed based on these output-input pairs. The regions of identified T_a is shown in Fig. 5. With the parameter vector $\alpha_{T_a}^i = [\alpha_1^i, \alpha_2^i, \alpha_3^i, \alpha_4^i]'$ and $[\omega_r(k), \theta(k), v_w(k)] \in \chi_{T_a}^i$, T_a at time step k can be expressed as,

$$T_a(k) = \alpha_1^i \omega_r(k) + \alpha_2^i \theta(k) + \alpha_3^i v_w(k) + \alpha_4^i. \tag{20}$$

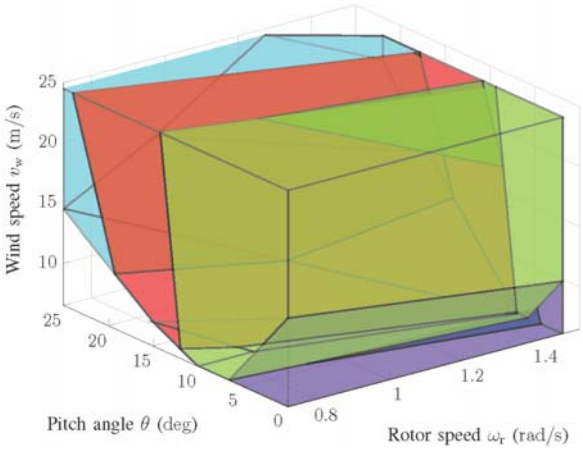

Fig. 5 Regions $\chi_{T_a}^i$ of T_a identification

B. Identification of generator torque T_g

The static nonlinear function for computing T_g is related to P_g^{cmd} and ω_g, which can further be transformed to be related to $P_{\text{ref}}^{\text{WT}}$ and ω_r. Therefore, the regressors shall be distributed in the two-dimensional space $[\omega_r, P_{\text{ref}}^{\text{WT}}]'$ bounded by the constraints. In this paper, 500 regressors are generated uniformly. With $s=4$ and $c=10$, the clustering-based identification is performed and the regions of identified T_g is shown in Fig. 6. With the parameter vector $\alpha_{T_g}^i = [\alpha_5^i, \alpha_6^i, \alpha_7^i]'$ and $[\omega_r(k), P_{\text{ref}}^{\text{WT}}(k)] \in \chi_{T_g}^i$, T_g at time step k can be derived,

$$T_g(k) = \alpha_5^i \omega_r(k) + \alpha_6^i P_{\text{ref}}^{\text{WT}}(k) + \alpha_7^i. \tag{21}$$

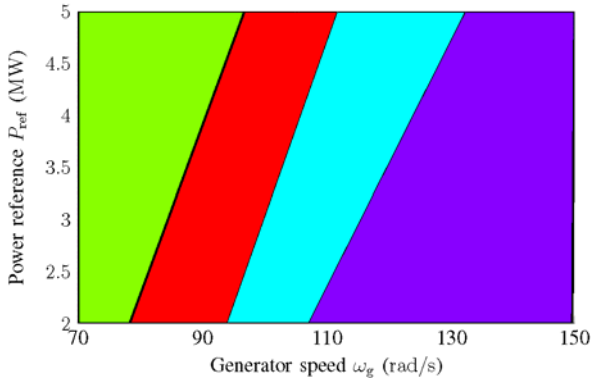

Fig. 6 Regions $\chi^i_{T_g}$ of T_g identification

C. Identification of thrust force F_t

The identification of F_t is similar to that of T_a. With the same regressor generation, the thrust force F_t to each regressor can be calculated according to (4) where C_t is obtained by interpolation of the look-up table in [19]. In this paper, s is set as 4 while c is set as 20. The corresponding regions of identified F_t is illustrated in Fig. 7. With the parameter vector $\alpha^i_{F_t} = [\alpha^i_8, \alpha^i_9, \alpha^i_{10}, \alpha^i_{11}]'$ and $[\omega_r(k), \theta(k), v_w(k)] \in \chi^i_{F_t}$, F_t at time step k can be derived,

$$F_t(k) = \alpha^i_8 \omega_r(k) + \alpha^i_9 \theta(k) + \alpha^i_{10} v_w(k) + \alpha^i_{11}. \quad (22)$$

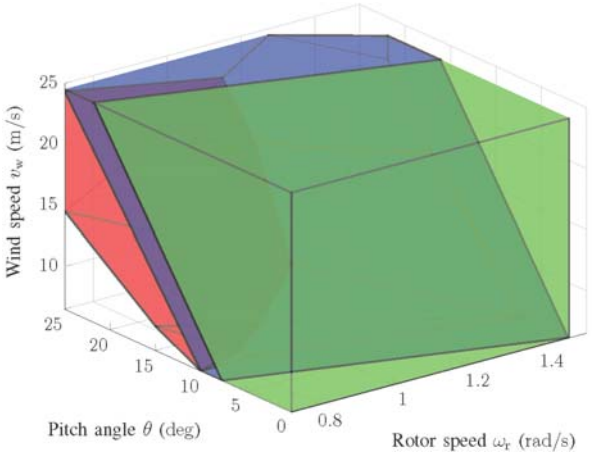

Fig. 7 Regions $\chi^i_{F_t}$ of F_t identification

D. Identification of correction factor K_c in pitch control

K_c is described as a function of P_{ref} and θ in (17). Different from the identification of the static nonlinear function, K_c is considered as a fixed value in a region, which avoids creating new nonlinearities. The parameter vector $\alpha^i_{K_c} = \alpha^i_{12}$, if $[P_{\text{ref}}(k), \theta(k)] \in \chi^i_{K_c}$. Accordingly,

$$K_c = \alpha^i_{12}. \quad (23)$$

In the NREL model, K_c applied in the gain-scheduling is only related to θ. By selecting $s = 4$, the range $[\theta_{\min}, \theta_{\max}]$ is equally divided into 4 segments.

E. Identification of the elements in A_d' and B_d' according to the constraint of $\dot{\theta}$ in pitch control

Let $M(m,n)$ represent the element of matrix M at m th row and n th column. According to (14) and (18), the discrete form of the pitch angle calculation is derived,

$$\theta(k+1) = A_d'(3,1)\cdot\omega_r(k) + A_d'(3,2)\cdot\omega_f(k) + A_d'(3,3)\cdot\theta(k) + B_d'(3,4)\cdot\omega_{\text{rated}} \quad (24)$$

The pitch angle difference between two steps $\Delta\theta$ can be expressed by,

$$\begin{aligned}\Delta\theta &= \theta(k+1) - \theta(k) \\ &= A_d'(3,1)\cdot\omega_r(k) + A_d'(3,2)\cdot\omega_f(k) + B_d'(3,4)\cdot\omega_{\text{rated}} - \theta(k)\end{aligned} \quad (25)$$

In order to fulfill the constraint $-\Delta\theta_{\max} \le \Delta\theta \le \Delta\theta_{\max}$, the space $[\omega_r(k), \omega_f(k), \theta(k)]$ can be partitioned into different regions according to $\Delta\theta$. In each region, the matrices A_d' and B_d' should be updated based on the following rules,

- If $\Delta\theta_{\max} < \Delta\theta$, $\theta(k+1) = \theta(k) + \Delta\theta_{\max}$. Then, $A_d'(3,1) = 0$, $A_d'(3,2) = 0$, $A_d'(3,3) = 1$, and $B_d'(3,4) = \dfrac{\Delta\theta_{\max}}{\omega_{\text{rated}}}$.
- If $\Delta\theta < -\Delta\theta_{\max}$, $\theta(k+1) = \theta(k) - \Delta\theta_{\max}$. Then, $A_d'(3,1) = 0$, $A_d'(3,2) = 0$, $A_d'(3,3) = -1$, and $B_d'(3,4) = -\dfrac{\Delta\theta_{\max}}{\omega_{\text{rated}}}$.

F. PWA model of a wind turbine

In order to include all the polytope regions identified above, a five dimensional space $[\omega_r, \omega_f, v_w, \theta, P^{\text{WT}}_{\text{ref}}]'$ is introduced. According to the operation areas, when the wind turbine operates in Area II, the pitch angle control is considered deactivated: $\theta = 0$. Therefore, only a three-dimensional space $[\omega_r, v_w, P^{\text{WT}}_{\text{ref}}]'$ is used. Each polytope regions constructed by the identification has to be intersected with others. In this case, the total number of all the intersected regions $\{\chi^i\}_{i=1}^{s_{\text{total}}}$ is $s_{\text{total}} = 47$.

For each region χ^i, the constant K_c is firstly brought into A in (18). Then, A_d' and B_d' are updated following the rules in Section V.E. According to (20)-(23), $g(k)$ can be expressed with the identified parameters,

$$g(k) = A_p x(k) + B_p u(k) + E_p d(k) + F_p \quad (26)$$

where

$$u = P_{\text{ref}}^{\text{WT}}, d = v_{\text{w}}, A_{\text{p}} = \begin{bmatrix} \alpha_1^i & 0 & \alpha_2 \\ \alpha_5^i & 0 & 0 \\ \alpha_8^i & 0 & \alpha_9^i \\ 0 & 0 & 0 \end{bmatrix},$$

$$B_{\text{p}} = \begin{bmatrix} \alpha_3^i \\ 0 \\ \alpha_{10}^i \\ 0 \end{bmatrix}, E_{\text{p}} = \begin{bmatrix} 0 \\ \alpha_6^i \\ 0 \\ 0 \end{bmatrix}, F_{\text{p}} = \begin{bmatrix} \alpha_4^i \\ \alpha_7^i \\ \alpha_{11}^i \\ \omega_{\text{rated}} \end{bmatrix}.$$

Accordingly, (22) can be transformed into a standard PWA format,

$$\begin{aligned} x(k+1) = \;& A_{\text{d}}x(k) + B_{\text{d}}u(k) + E_{\text{d}}d(k) + F_{\text{d}} \\ y(k) = \;& C_{\text{d}}x(k) + D_{\text{d}}u(k) + G_{\text{d}}d(k) + H_{\text{d}} \\ \text{if} \; & \begin{bmatrix} x(k) \\ u(k) \\ d(k) \end{bmatrix} \in \chi^i. \end{aligned} \tag{27}$$

where

$$A_{\text{d}} = A_{\text{d}}' + B_{\text{d}}'A_{\text{p}}, B_{\text{d}} = B_{\text{d}}'B_{\text{p}}, E_{\text{d}} = B_{\text{d}}'E_{\text{p}}, F_{\text{d}} = B_{\text{d}}'F_{\text{p}},$$
$$C_{\text{d}} = C_{\text{d}}' + D_{\text{d}}'A_{\text{p}}, D_{\text{d}} = D_{\text{d}}'B_{\text{p}}, G_{\text{d}} = D_{\text{d}}'E_{\text{p}}, H_{\text{d}} = D_{\text{d}}'F_{\text{p}}.$$

VI. Case Study

In this section, the case study results are presented and compared with these of the 5 MW NREL nonlinear wind turbine model. The PWA modeling and simulation were executed in a Matlab toolbox-Multi-Parametric Toolbox (MPT) [27], [28]. The simulation time of both cases is 300 s. Two scenarios were used to test the developed PWA model of the wind turbine under the high and low wind conditions. Besides, the power reference is also varying during simulation, as illustrated in Fig. 8, which has two step changes at $t = 100\text{s}$ and $t = 200\text{s}$, respectively.

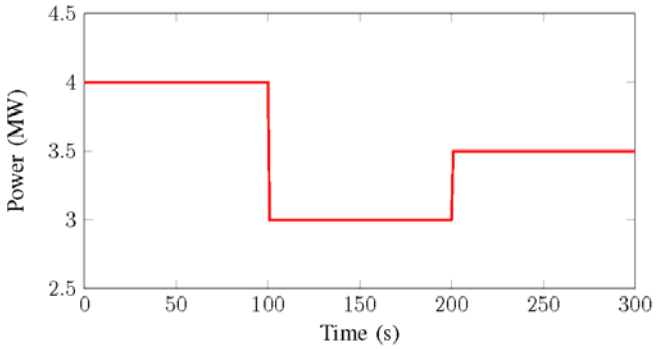

Fig. 8 Power reference

A. Low wind speed case

The wind speed profile of this case is shown in Fig. 9, which covers the range between 10 m/s and 15 m/s. The simulation results of both PWA model (PWA) and nonlinear NREL model (NL) are illustrated and compared in Fig. 10 and Fig. 11, including system states (θ and ω_{r}) and outputs (T_{s}, F_{t}).

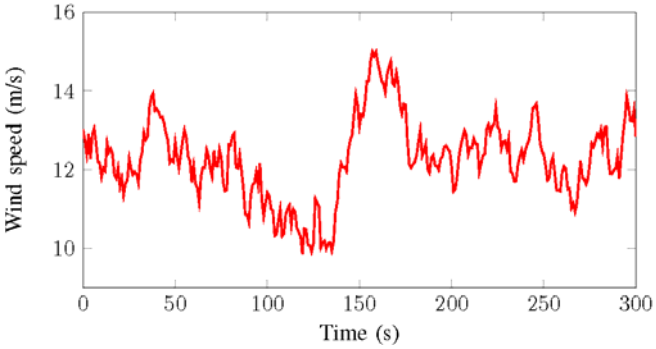

Fig. 9 Wind speed variation in the low speed condition

(a)

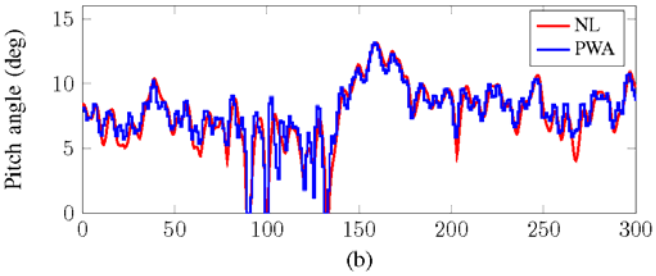

(b)

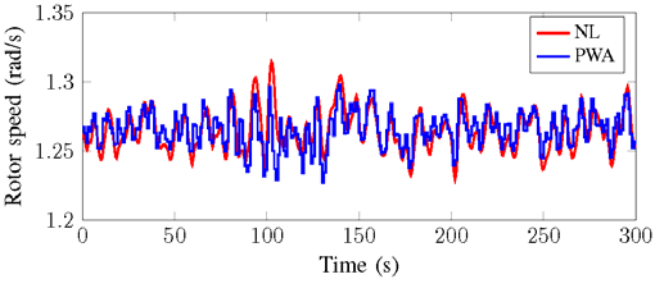

Fig. 10 State variable comparison

(a)

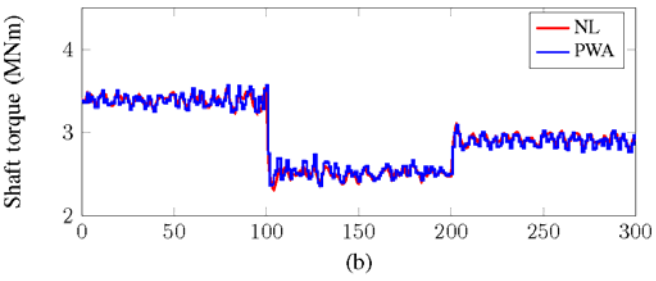

(b)

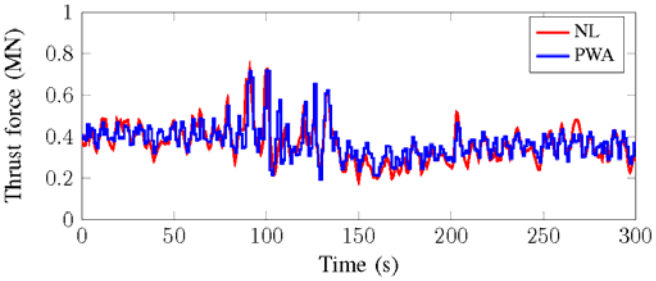

Fig. 11 Output variable comparison

The pitch angle θ varies following the wind variation to regulate the power production. When the pitch angle is reduced to $\theta = 0$, the system will get into Area II. Accordingly, the pitch angle control is deactivated. Otherwise, the rotor speed ω_r is regulated to avoid the rotor from over-speeding. The rated rotor speed value $\omega_{rated} = 1.2671$. The shaft torque is basically follows the variation of the power reference. Percentage Root Mean Square Error (%RMSE) is commonly used to evaluate the model mismatch. The lower the %RMSE is, the better the model performance is. The %RMSE values of θ, ω_r, T_s, F_t in the low wind speed case are listed in Table I. The maximum %RMSE value is 9.8916 which is lower than the commonly used threshold of 10. It shows a good agreement between these two models which verifies the developed PWA model in the low wind condition.

TABLE I
SIMULATION STATISTICS %RMSE

	θ	ω_r	T_s	F_t
Low Wind	5.5827	1.0283	2.1631	9.8316

The reason of the error is twofold. Firstly, the model has been simplified and some dynamics are ignored, as described in Section IV. Secondly, in order to reduce the complexity of the PWA model, the number of sub-models is limited which reduces the approximation accuracy. However, this error will not significantly affect the wind farm control performance. The simulation time in this case is set 5 min, while in the real-time MPC control, the prediction horizon is much shorter than this range, normally in several seconds. Besides, the prediction error can be compensated by the feedback mechanism.

B. *High wind speed case*

A similar procedure was used for the high wind speed case. The same wind profile is shifted upwards and the speed range covers between 15 m/s and 20 m/s, as shown in Fig. 12. The simulation results of both the PWA model (PWA) and the nonlinear NREL model (NL) are illustrated and compared in Fig. 13 and Fig. 14, including system states (θ and ω_r) and outputs (T_s, F_t).

The pitch angle θ changes following the wind speed variation to regulate the power production. The pitch angle control is always in the active state (Area I). Rotor speed ω_r is regulated around its rated value 1.2671. The shaft torque is basically follows the variation of the power reference. The range of %RMSE values listed in Table II is between 0.8070 and 7.7993, which shows a better agreement of these two models than that in the low wind condition.

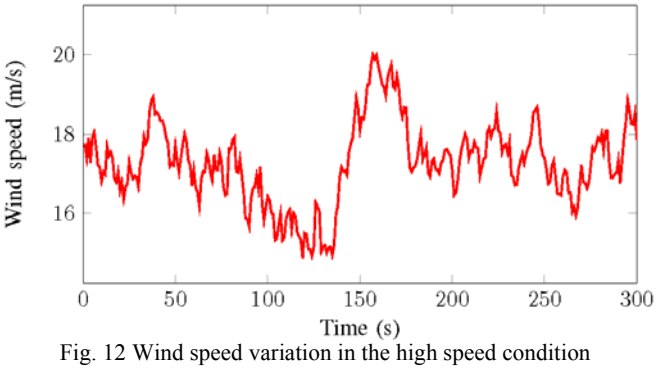

Fig. 12 Wind speed variation in the high speed condition

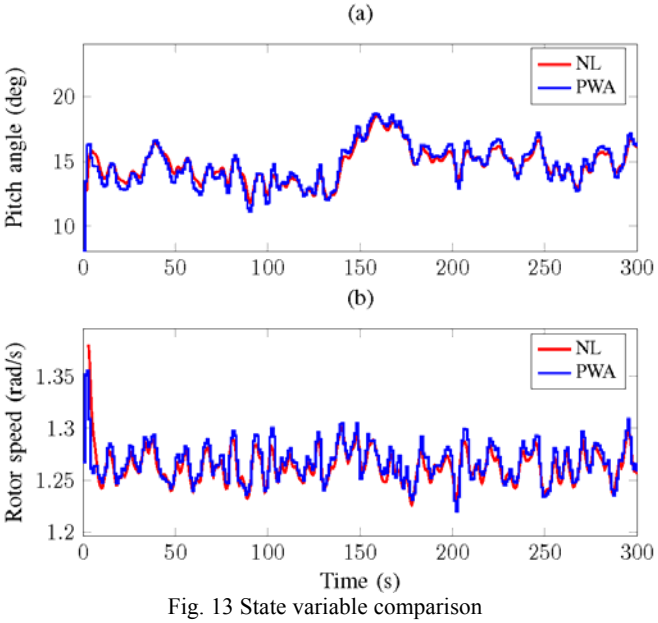

Fig. 13 State variable comparison

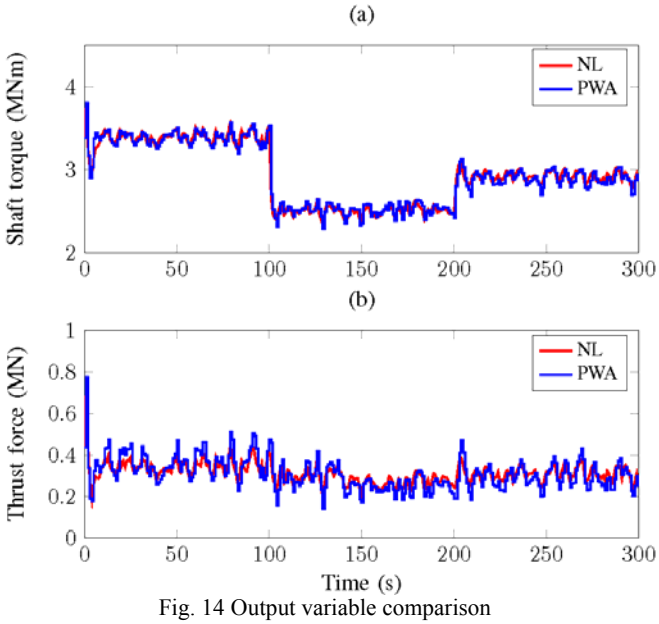

Fig. 14 Output variable comparison

TABLE II
SIMULATION STATISTICS %RMSE

	θ	ω_r	T_g	F_t
High Wind	3.8706	0.8070	1.6585	7.7993

VII. CONCLUSION

A dynamic discrete-time PWA model of a power controlled wind turbine is developed in this paper for the optimal active power control of a wind farm. The nonlinearities are identified by the clustering-based identification method. Compared with the linearization at some selected operating points, it has advantages to estimate the linear sub-models by classifying the multidimensional operating points and reconstructing the regions optimally. By comparison with the nonlinear model, the developed model is validated under both high and low wind conditions with different power references. All the state variables are measurable or estimated. Due to its simplicity, the developed PWA model is suitable for the advanced optimal control at the wind farm level, including the MPC (centralized or distributed) and the LQR.

VIII. REFERENCES

[1] European Wind Energy Association, "Wind in power, 2013 european statistics, 2013," [Online]. Available: http://www.ewea.org/fileadmin/files/library/publications/statistics/EWEA_Annual_Statistics_2013.pdf.

[2] M. Tsili and S. Papathanassiou, "A review of grid code technical requirements for wind farms," *IET Renew. Power Gen.*, vol. 3, no. 3, pp. 308–332, 2009.

[3] P. E. Sørensen, A. D. Hansen, F. Iov, F. Blaabjerg, and M. H. Donovan, "Wind farm models and control strategies," Risø National Laboratory, Tech. Rep., Risø-4-1464, Aug. 2005.

[4] A. D. Hansen and G. Michalke, "Multi-pole permanent magnet synchronous generator wind turbines' grid support capability in uninterrupted operation during grid faults," *IET Renew. Power Gen.*, vol. 3, no. 3, pp. 333–348, 2009.

[5] Z. Chen, J. M. Guerrero, and F. Blaabjerg, "A review of the state of the art of power electronics for wind turbines," *IEEE Trans. Power Electron.*, vol. 24, no. 8, pp. 1859–1875, 2009.

[6] D. Madjidian, K. Martensson, and A. Rantzer, "A distributed power coordination scheme for fatigue load reduction in wind farms," in *Proc. 2011 IEEE American Control Conf. (ACC)*, pp. 5219–5224.

[7] B. Biegel, D. Madjidian, V. Spudic, A. Rantzer, and J. Stoustrup, "Distributed low-complexity controller for wind power plant in derated operation," in *Proc. 2013 IEEE International Conf. on Control Applications (CCA)*, pp. 146–151.

[8] V. Spudić, M. Jelavic, M. Baotic, and N. Peric, "Hierarchical wind farm control for power/load optimization," in *Proc. 2010 The Science of making Torque from Wind (Torque2010)*.

[9] V. Spudić, M. Jelavić, and M. Baotić, "Wind turbine power references in coordinated control of wind farms," *Automatika–Journal for Control, Measurement, Electronics, Computing and Communications*, vol. 52, no. 2, 2011.

[10] Y.-T. Shi, Q. Kou, D.-H. Sun, Z.-X. Li, S.-J. Qiao, and Y.-J. Hou, "H ∞ fault tolerant control of wecs based on the PWA model," *Energies*, vol. 7, no. 3, pp. 1750–1769, 2014.

[11] M. Soliman, O. P. Malik, and D.T. Westwick, "Multiple model predictive control for wind turbines with doubly fed induction generators," *IEEE Trans. Sustain. Energy,* vol. 2, no. 3, pp. 215-225, 2011.

[12] S. Paoletti. "Identification of piecewise affine models," PhD thesis, University of Siena, Siena, Italy, 2004.

[13] P. Julian, A. Desages, O. Agamennoni, "High-level canonical piecewise linear representation using a simplicial partition," IEEE Trans. Circuits Syst. I, Fundam. Theory Appl., vol. 46, no. 4, pp. 463-480, 1999.

[14] T.A. Johansen, B.A. Foss, "Identification of non-linear system structure and parameters using regime decomposition," *Automatica*, vol. 31, no. 2, pp. 321-326, 1995.

[15] A. Bemporad, J. Roll, and L. Ljung, "Identification of hybrid systems via mixed-integer programming," in *Proc. 1998 IEEE Conference on Decision and Control*, pp. 786-792.

[16] J. Roll, A. Bemporad, and L. Ljung, "Identification of piecewise affine systems via mixed-integer programming," *Automatica*, vol 40, pp. 37-50.

[17] G. Ferrari-Trecate, M. Muselli, D. Liberati, and M. Morari, "A clustering technique for the identification of piecewise affine systems," *Automatica*, vol. 39, no. 2, pp. 205–217, 2003.

[18] M. Vasak, N. Hure, and N. Peric, "Identification of a discrete-time piecewise affine model of a pitch-controlled wind turbine," in *Proc. 2011 the 34th International Convention*, pp. 744–749.

[19] J. Jonkman, S. Butterfield, W. Musial, and G. Scott, "Definition of a 5 MW reference wind turbine for offshore system development," National Renewable Energy Laboratory, Tech. Rep., 2009.

[20] J.D. Grunnet, M. Soltani, T. Knudsen, et al. "Aeolus toolbox for dynamics wind farm model, simulation and control", *European Wind Energy Conference & Exhibition, EWEC 2010.*

[21] H. Zhao, Q. Wu, C. Rasmussen, and M. Blanke, "L1 adaptive speed control of a small wind energy conversion system for maximum power point tracking, " *IEEE Trans. on Energy Conv.*, vol. 29, no. 3, pp. 576–584, Sept. 2014.

[22] Y. Xue, N. Tai, "Review of contribution to frequency control through variable speed wind turbine," *Renewable Energy,* vol. 36, no. 6, pp. 1671-1677, 2011.

[23] L. Holdsworth, J.B. Ekanayake, N. Jenkins, "Power system frequency response from fixed speed and doubly fed induction generator based wind turbines," *Wind energy,* vol. 7, no. 1, pp. 21-35, 2004.

[24] G. Ferrari-Trecate, "Hybrid Identification Toolbox (HIT)," Tech. Rep., 2005.

[25] I. Munteanu, A.I. Bratcu, N.A. Cutululis, et al, *Optimal control of wind energy systems: towards a global approach*. Springer, 2008.

[26] J. M. Maciejowski, *Predictive control: with constraints*. Pearson education, 2002.

[27] J. Lunze and F. Lamnabhi-Lagarrigue, *Handbook of hybrid systems control: theory, tools, applications*. Cambridge University Press, 2009.

[28] M. Herceg, M. Kvasnica, C. Jones, and M. Morari, "Multi-Parametric Toolbox 3.0," in *Proc. 2013 European Control Conf.*, pp 502-510.

IX. BIOGRAPHIES

Haoran Zhao received the B.E from Shandong University, China, in 2005, the M.E. degree from Technical University of Berlin, Germany in 2009 and the PhD from Technical University of Denmark in 2015. He is a PostDoc the Center for Electric Technology, Technical University of Denmark, Denmark. He worked as Electrical Engineer in State Grid Corporation of China (SGCC) shortly in 2005. From Aug. 2010 to Sep. 2011, he worked as Application Developer in DIgSILENT GmbH, Germany. His research interests are modeling and integration study of wind power, control of energy storage system and voltage stability analysis.

Qiuwei Wu (M'08**)** obtained the B. Eng. and M. Eng. from Nanjing University of Science and Technology, Nanjing, P. R. China, in 2000 and 2003, respectively, both in Power System and Automation. He obtained the PhD degree from Nanyang Technological University, Singapore, in 2009, in Power System Engineering.

He was a senior R&D engineer with VESTAS Technology R&D Singapore Pte Ltd from Mar. 2008 to Oct. 2009. He was a PostDoc with Centre for Electric Technology (CET), Department of Electrical Engineering, Technical University of Denmark (DTU) from Nov. 2009 to Oct. 2010, an Assistant Professor from Nov. 2010 to Aug. 2013 and has been an Associate Professor since Sept. 2013 with the same centre.

Qinglai Guo (SM'2014) was born in Jilin City, Jilin Province in China on Mar. 6, 1979. He graduated from the Department of Electrical Engineering, Tsinghua University, Beijing, China, in 2000 with B.S degree. He received his PhD degree from Tsinghua University in 2005 where he is now an associate professor. He is a member of CIGRE C2.13 Task Force on Voltage/Var support in System Operations. His special fields of interest include smart grids, cyber-physical systems and electrical power control center applications.

Hongbin Sun (SM' 2012) received his double B.S. degrees from Tsinghua University in 1992, the Ph.D from Dept. of E.E., Tsinghua University in 1997. He is now Changjiang Scholar of Education Ministry of China, full professor of electrical engineering in Tsinghua Univ. and assistant director of State Key Laboratory of Power Systems in China. From 2007.9 to 2008.9, he was a visiting professor with School of EECS at the Washington State University in Pullman. He is a Fellow of IET. He is a member of IEEE PES CAMS Cascading Failure Task Force and CIGRE C2.13 Task Force on Voltage/Var support in System Operations. In recent 15 years, he led a research group in Tsinghua University to develop a commercial system-wide automatic voltage control systems, which has been applied to PJM interconnection, the largest regional power grid in USA, and to more than 60 large-scale power grids in China. He published more than 300 academic papers. He won the China National Technology Innovation Award in 2008, the National Distinguished Teacher Award in China in 2009, and the National Science Fund for Distinguished Young Scholars of China in 2010. His research interests include smart grids, renewable generation integration, and electrical power control center applications.

Yusheng Xue received MSc degree in Electrical Engineering from EPRI, China in 1981 and PhD degree from the University of Liege, Belgium in 1987. He was elected as an academician of Chinese Academy of Engineering in 1995. He is now the Honorary President of State Grid Electric Power Research Institute (SGEPRI or NARI), China. He holds the positions of Adjunct Professor in many universities in China and a conjoint professor of the University of Newcastle in Australia. He is also an honorary professor of the University of Queensland, Australia. He has been a member of the PSCC Council, and the Editor-in-Chief of Automation of Electric Power System since 1999, and a member of Editorial Board of IET Generation, Transmission & Distribution, and Chairman of Technical Committee of Chinese National Committee of CIGRE since 2005.